Numerical Study of Oblique Shock Wave

Amir Hussein Ali

Department of Physics, College of Education for Pure Science, University of Basrah, Basra, Iraq.

*Corresponding author E-mail: amir.ali@uobasrah.edu.iq

Doi:10.29072/basjs.20230106

ARTICLE INFO

Keywords

Oblique shock wave, Fluid flow, Computational fluid dynamics.

ABSTRACT

This study aims to investigate some physical parameters in presence of an oblique shock wave numerically. Computational fluid dynamics has been used to analyze fluid behavior upstream and downstream of the shock wave. To obtain a good resolution, the computational domain is constructed by fine meshing. Due to its wide use in engineering applications, Air has been used as fluid material. A wedge of half-angle $\theta = 22°$ has been used to intercept the airflow path and founding the oblique shock wave of angleϕ. For gathering comprehensive information, the air flows have been tested for three Mach numbers, namely slightly higher than 1, slightly higher than two, and slightly higher than three (M1~=1, M2~=2, and M3~=3) and represented as a case (a), (b) and (c) respectively. The continuity equation, momentum equation, and energy equation have been solved numerically. Velocity, turbulent viscosity, total pressure, and total enthalpy have been investigated upstream and downstream of the shockwave for the three different Mach numbers. The results showed that the total pressure downstream of the shock wave was less than that of the upstream shock wave. In addition, the turbulent viscosity area around the object becomes thicker as the Mach numbers become bigger. Also, the total pressure was slightly different for the three different Mach numbers. These behaviors of the above-mentioned parameters are attributed to the shock wave effects. In addition, the oblique shock wave angle ϕ is appeared to be decreased as the Mach number increased.

Received 22 Jun 2022; Received in revised form 23 Oct 2022; Accepted 12 Feb 2023, Published 30 Apr 2023

This article is an open access article distributed under the terms and conditions of the Creative Commons Attribution-NonCommercial 4.0 International (CC BY-NC 4.0 license) (http://creativecommons.org/licenses/by-nc/4.0/).

1. Introduction

In supersonic airflow, an oblique shock wave of angle ϕ will be constructing in case a wedge of half-angle θ intercept the airflow as illustrated in **Error! Reference source not found.**.

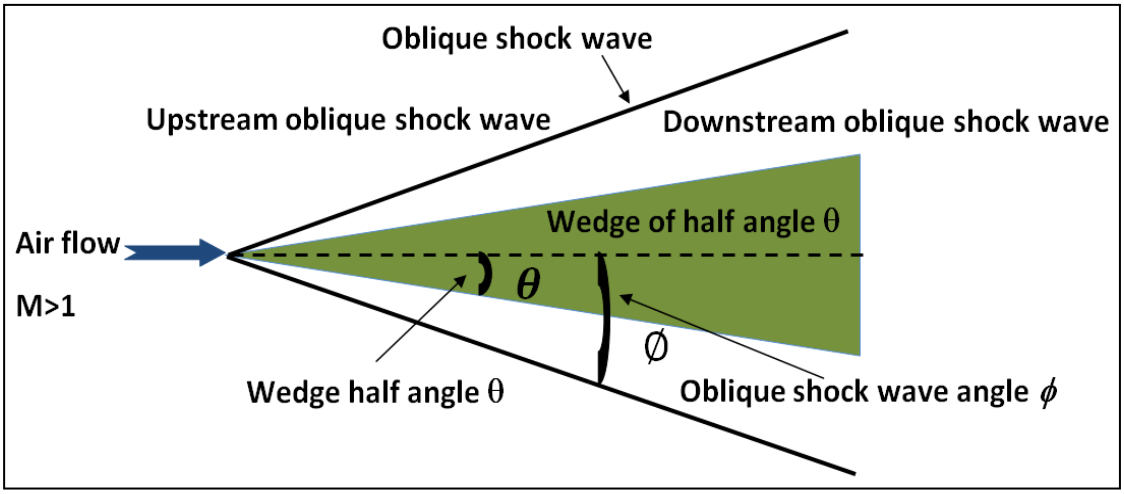

Figure 1: Oblique shock wave sketch.

The oblique shock wave is created because of an abrupt decrease in the airflow. The shock wave area is a very small region in the air where the air properties change significantly. Two cases of oblique shock waves of two different angles are possible. The oblique shock wave of a large angle ϕ is called a strong shock wave while that of a small angle ϕ is called a weak shock wave. On the two sides of the oblique shock wave the equations which describe the change in the airflow variables are as follow [1]:

$$\boldsymbol{\cot\theta = \tan\emptyset\left[\frac{(\gamma+1)M^2}{2(M^2\sin^2\emptyset-1}-1\right]} \quad (1)$$

$$\boldsymbol{\frac{T_1}{T_o} = \frac{[2\gamma M^2\sin^2\emptyset-(\gamma-1)]\,[(\gamma-1)M^2\sin^2\emptyset+2]}{(\gamma+1)^2M^2\sin^2\emptyset}} \quad (2)$$

$$\boldsymbol{\frac{P_{t1}}{P_{to}} = \left[\frac{(\gamma+1)M^2\sin^2\emptyset}{(\gamma-1)M^2\sin^2\emptyset+2}\right]^{\frac{\gamma}{\gamma-1}}\left[\frac{(\gamma+1)}{2\gamma M^2\sin^2\emptyset-(\gamma-1)}\right]^{\frac{1}{\gamma-1}}} \quad (3)$$

$$\boldsymbol{M_1^2\sin^2(\emptyset-\theta) = \frac{(\gamma-1)M^2\sin^2\emptyset+2}{2\gamma M^2\sin^2\emptyset-(\gamma-1)}} \quad (4)$$

This article is an open access article distributed under the terms and conditions of the Creative Commons Attribution-NonCommercial 4.0 International (CC BY-NC 4.0 license) (http://creativecommons.org/licenses/by-nc/4.0/).

$$\frac{P_1}{P_0} = \frac{2\gamma M^2 sin^2\emptyset - (\gamma - 1)}{(\gamma - 1)} \quad (5)$$

$$\frac{\rho_1}{\rho_0} = \frac{(\gamma+1)M^2 sin^2\emptyset}{(\gamma-1)M^2 sin^2\emptyset + 2} \quad (5)$$

where T_o, M_o and P_{to} are the temperature, Mach number, and total pressure upstream of the oblique shock wave respectively, while T_1, M_1, and P_{t1} are the same variables downstream of the oblique shock wave. In addition, γ is the specific heat ratio. Due to its widespread in engineering applications, the shock wave has studded intensively in different engineering areas [2], [3], [4], [5]. Moreover, because of their importance in aeronautical applications, recently shock wave has gained inevitable significance. Also, shock wave boundary layer interaction received great attention in the high-speed aeronautic area. [6] investigated the normal shock wave boundary layer numerically. [7] studied the correlations for shock wave boundary layer interaction by use of numerical technique using an in-house solver. The modifications suggested are seen to improve the applicability of the existing correlations. [8] studied the effects of unsteady oblique shock waves on the mixing efficiency of a two-dimensional supersonic mixing layer. They used direct numerical simulation. The effects of three conditions on the mixing efficiency of the mixing layer have been performed. Their results indicated that the mixing layer is affected by the shock wave. [9] studied the detonations in condensed phase explosives and they investigated the oblique shock waves in the surrounding fluids. Fluid material was considered an ideal gas. Their study was conducted numerically. Depending on the specific heat ratio, they observed four structures behind the oblique shock wave. [10] obtained numerical simulation boundary condition based on outburst characteristics. The propagation characteristics of shock wave and gas flow were performed numerically. They concluded that the air shock wave was formed because of air medium was compressed by transient high-pressure gas which expands in the roadway strongly. Also, the gas flow of high velocity and the shock wave was constructed behind the shock wavefront. [11] had constructed a method of multi-shock wave system to improve turbine reliability. The grooved surface nozzle was investigated. They concluded that in the multi-shockwave system the intensity of the shock wave is weakened compared to the single normal shock wave and hence the impact on the turbine wheel will be less effective. It could be noted that the oblique shock wave occurs in various engineering configurations as in over-expanded nozzles or the supersonic aircraft's inlet. [12] presented experimental results of shock wave/turbulent boundary layer interaction. Strong unsteadiness was developing inside the separated zone. They concluded the feasibility

This article is an open access article distributed under the terms and conditions of the Creative Commons Attribution-NonCommercial 4.0 International (CC BY-NC 4.0 license) (http://creativecommons.org/licenses/by-nc/4.0/).

of the spatial-time correlation between wall pressure and velocity in the shock wave turbulent boundary layer for compressible flow. [13] proposed a simple theoretical approach to determine a complicated oblique shock wave of internal flow with supersonic inflow boundary conditions. The main conclusion was that the predicted results of the incident shock wave at several inlet conditions were in good agreement with the results of the numerical simulations.

2. Procedure

In this study, computational fluid dynamics (CFD) has been used to investigate the oblique shock wave using air as fluid material. The computational domain has been constructed at 4 m in length, while the inlet and outflow height were 0.5 m and 1 m respectively. The deflection angle of the flow has been created by use of a wedge of half-angle θ = 22° and has been used to intercept the airflow path and founding the oblique shock wave of angleϕ as illustrated in Figure 2. The air flows have been tested for three different Mach numbers, namely slightly higher than one, slightly higher than two, and slightly higher than three, (M1~=1, M2~=2, and M3~=3) and represented as cases A, B, and C respectively. To obtain a good resolution, the computational domain is constructed with fine meshing. To perform the simulation, the momentum conservation equation, continuity equation, and energy equation have been solved numerically. The mathematical form of conservation of momentum is given as follows:

$$\frac{\partial}{\partial t}(\rho\vec{v}) + \nabla.(\rho\vec{v}\,\vec{v}) = -\nabla p + \nabla(\bar{\bar{\tau}}) + \rho\vec{g} + \vec{F} \qquad (6)$$

where p and ρ are the static pressure and the density respectively.

$\bar{\bar{\tau}}$ is the stress tensor, while $\rho\vec{g}$ and $\vec{F}$ are the gravitational body force and external body forces respectively.

Also, the stress tensor $\bar{\bar{\tau}}$ is represented as in equation 8.

$$\bar{\bar{\tau}} = \mu[(\nabla\vec{v} + \nabla\vec{v}^{T}) - \frac{2}{3}\nabla.\vec{v}\,I] \qquad (7)$$

where μ denotes the molecular viscosity, and I denote the unit tensor.

In the current study, the continuity equation has been solved numerically. The continuity equation states that the rate of fluid mass which inter the control volume is equal to that which leaves the control volume adding to the accumulation of mass within the system. Hence continuity equation is called the equation for conservation of mass. The equation for conservation of mass, or continuity equation, can be written as follows:

$$\frac{\partial \rho}{\partial t} + \nabla\ .\ (\rho\,\vec{v}) = S_m \qquad \mathbf{(8)}$$

This article is an open access article distributed under the terms and conditions of the Creative Commons Attribution-NonCommercial 4.0 International (CC BY-NC 4.0 license) (http://creativecommons.org/licenses/by-nc/4.0/).

where ρ and ν are the density and velocity of the fluid respectively, while *Sm* is the mass added to the continuous phase from the dispersed second phase.

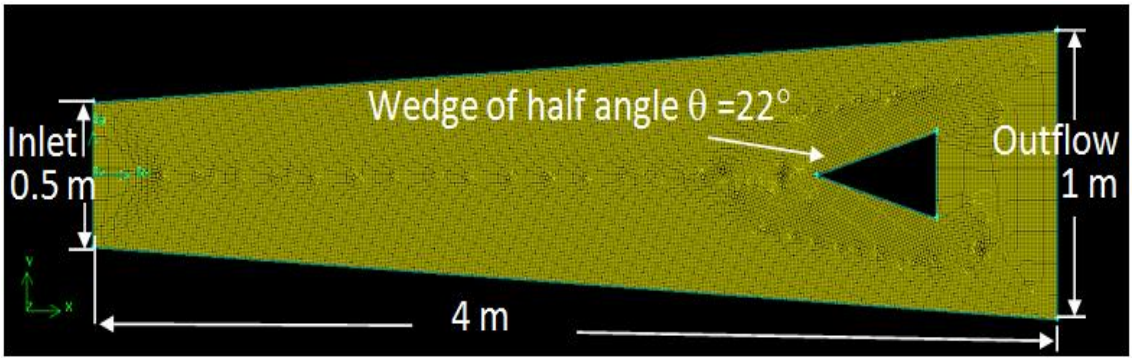

To

Figure 2: represent the computational domain.

present the thermal development across the oblique shock wave, the energy equation has been solved numerically. The general energy equation is given as in equation 10.

$$\frac{\partial}{\partial t}(\rho h) + \nabla \cdot (\vec{v}\rho h) = \nabla \cdot (k\nabla T) + S_h \qquad (9)$$

Where ρ, h, S_h, $\vec{v}$ and k are the density, enthalpy, volumetric heat source, velocity, and thermal conductivity respectively.

3.Results and discussion

Measurements of velocity behavior and velocity magnitude have been performed for the three different Mach numbers, case (a), case (b), and case(c) as illustrated in Figure 3. As expected, it can be shown that as the Mach number increased, the oblique shock wave angle ϕ decreased. This result is consistent with the analytical solution where for a given Mach number, the wave angle takes a range of possible values [1]:

$$\sin^{-1}\frac{1}{M} \leq \phi \leq \frac{\pi}{2}$$

For each value of θ and Mach number M, there are two possible solutions of ϕ, large and small value. The large value gives the stronger oblique shock wave and the flow becomes subsonic downstream of the oblique shock wave while the small value results in a weak oblique shock wave and the flow remains supersonic downstream of the oblique shock wave. The current investigation shows that the oblique shock wave is weak and the flow downstream has remained supersonic for the three cases as illustrated in Figure 3. This behavior has been emphasized by the total pressure investigation for the three cases as illustrated in Figure 4. The total pressure

This article is an open access article distributed under the terms and conditions of the Creative Commons Attribution-NonCommercial 4.0 International (CC BY-NC 4.0 license) (http://creativecommons.org/licenses/by-nc/4.0/).

near the wedge reached its maximum value at a distance of 3.5 m from the inlet flow to consist of a total pressure peak for each case. Furthermore, the maximum value of the total pressure near the wedge of case a was less than that of case b, and the latter was less than the total pressure of case c. Beyond the pressure peak, the total pressure decreased until reaching near 4m and try to raise again. This raising has become clearer and increases as the Mach number is increased as can be seen for the three cases in the plot of Figure 4. The vorticities became stronger as the Mach number increased and certainly can contribute to many interactions which in turn can change the total pressure value. The measurements of total enthalpy show similar behavior to the total pressure i.e. a total enthalpy peak has appeared at a distant 3.5 m from the inlet flow as illustrated in the plot of Figure 5. It should be noted that as the Mach number increased, the total enthalpy peak value become higher. Furthermore, the behavior of the total enthalpy down the peak is not affected because of the conservation of energy. The total enthalpy simulation has been illustrated in Figure 6. It can be seen that the less enthalpy occurred is behind the wedge for all the cases with little differences because of different Mach numbers, in turn, stimulate more vorticities as the Mach number has increased. The effect of oblique shock waves on the fluid flow became more evident by investigating the turbulent viscosity of the fluid flow across the wedge. The simulation of turbulent viscosity has been illustrated in Figure 7. It can be seen that the turbulent viscosity area in the shock wave region becomes thicker as the Mach number increases. This result is agreed well with the total pressure and total enthalpy results. However, the influence of the viscosity drag force decreases due to the increase in the airflow velocity but the influence of the form drag force caused by the pressure increases. As flow velocity increases, the onset of eddy currents will increase and the boundary layer will change to a turbulent boundary layer. Furthermore, the turbulence appears due to either increase in fluid flow velocity or an increase in surface roughness of the front surface wedge submerged into the airflow.

This article is an open access article distributed under the terms and conditions of the Creative Commons Attribution-NonCommercial 4.0 International (CC BY-NC 4.0 license) (http://creativecommons.org/licenses/by-nc/4.0/).

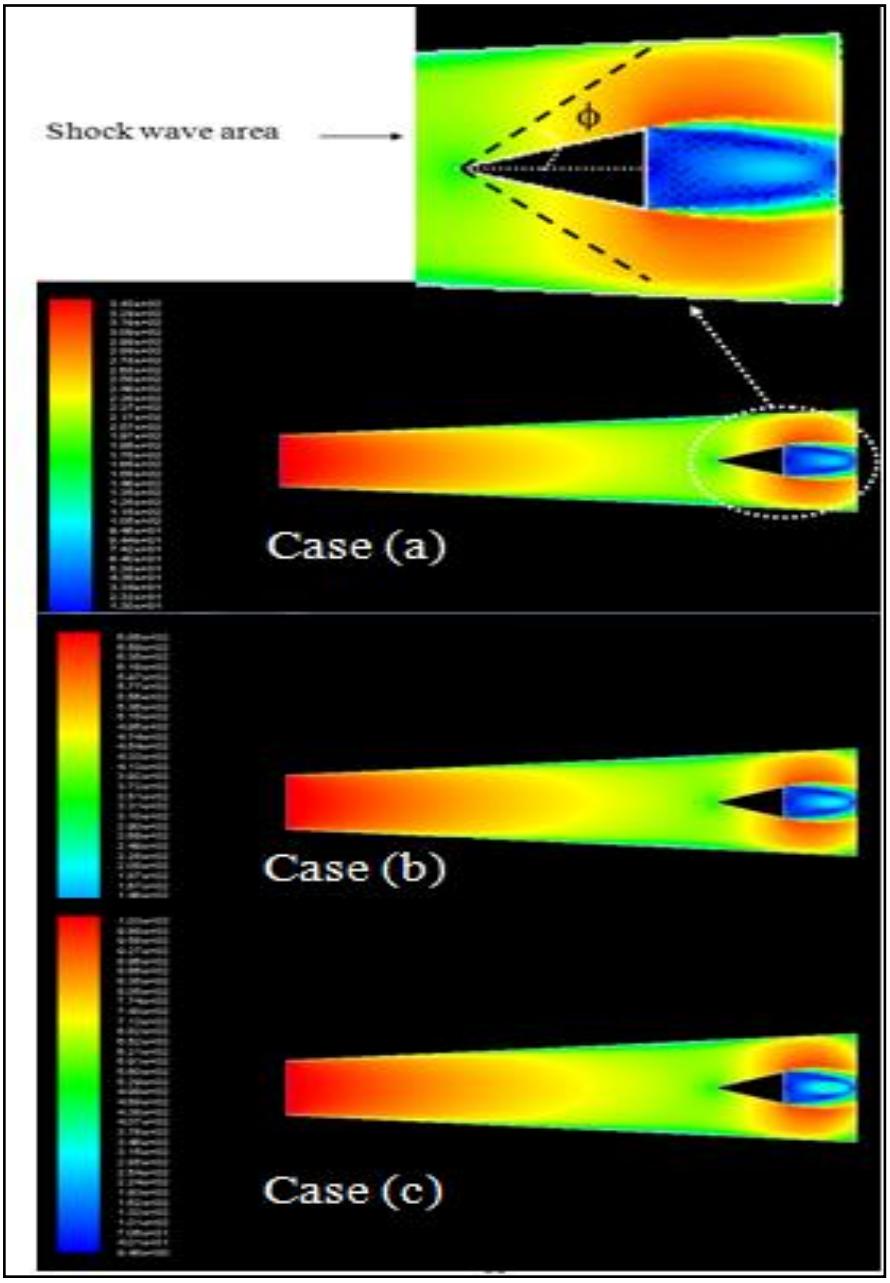

Figure 3: Velocity simulation of the three cases.

This article is an open access article distributed under the terms and conditions of the Creative Commons Attribution-NonCommercial 4.0 International (CC BY-NC 4.0 license) (http://creativecommons.org/licenses/by-nc/4.0/).

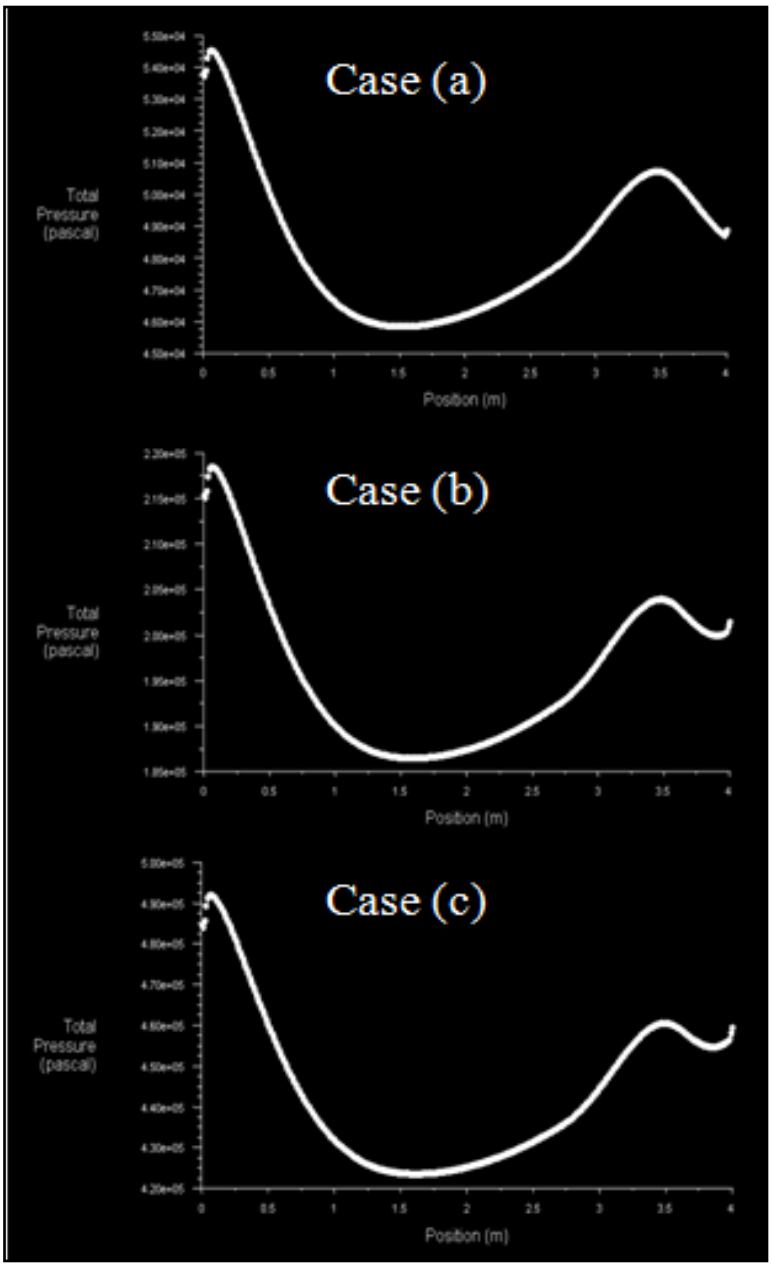

Figure 4: Total pressure plot of the three cases.

This article is an open access article distributed under the terms and conditions of the Creative Commons Attribution-NonCommercial 4.0 International (CC BY-NC 4.0 license) (http://creativecommons.org/licenses/by-nc/4.0/).

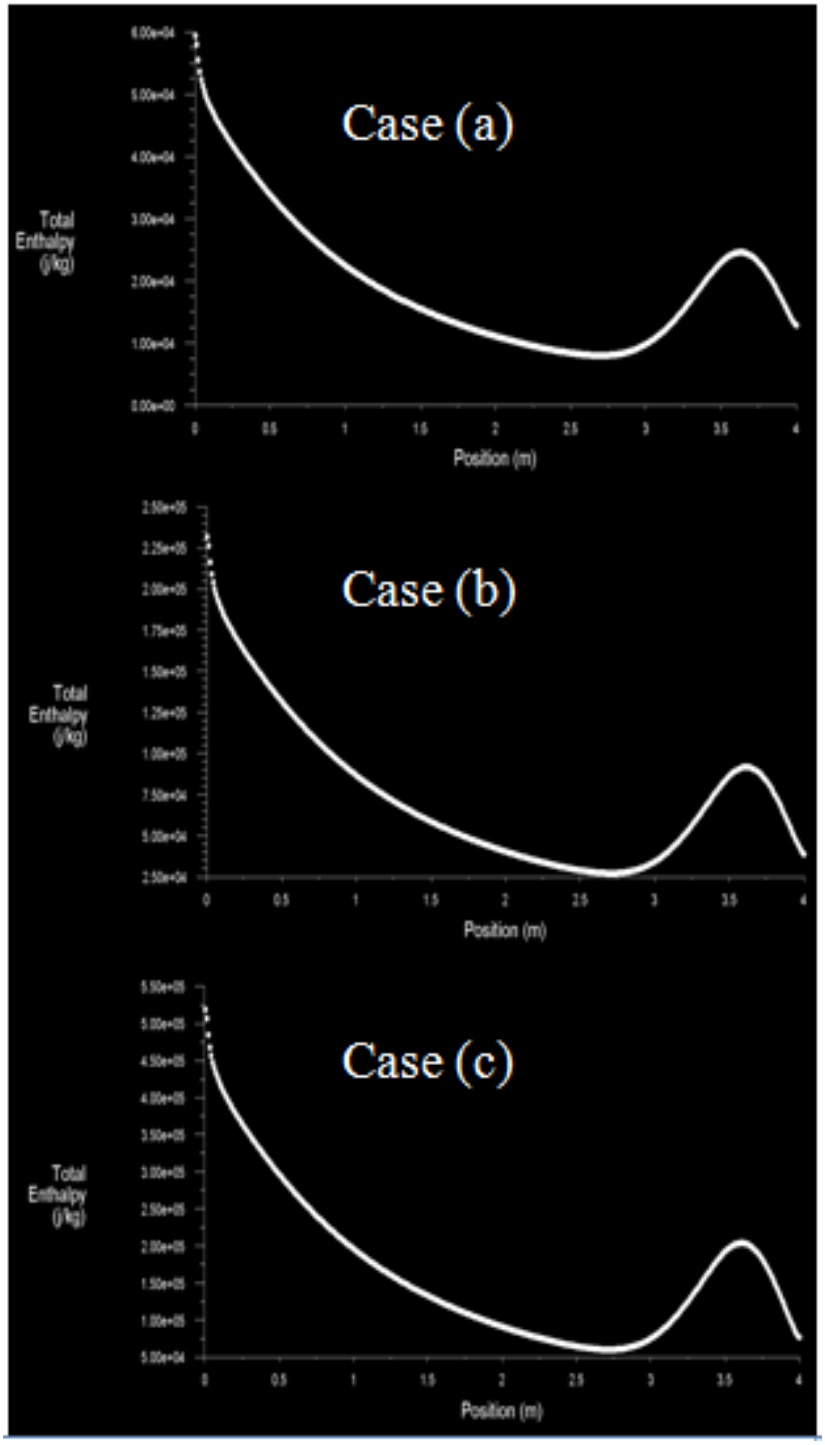

Figure 5. Total Enthalpy plot of the three cases.

This article is an open access article distributed under the terms and conditions of the Creative Commons Attribution-NonCommercial 4.0 International (CC BY-NC 4.0 license) (http://creativecommons.org/licenses/by-nc/4.0/).

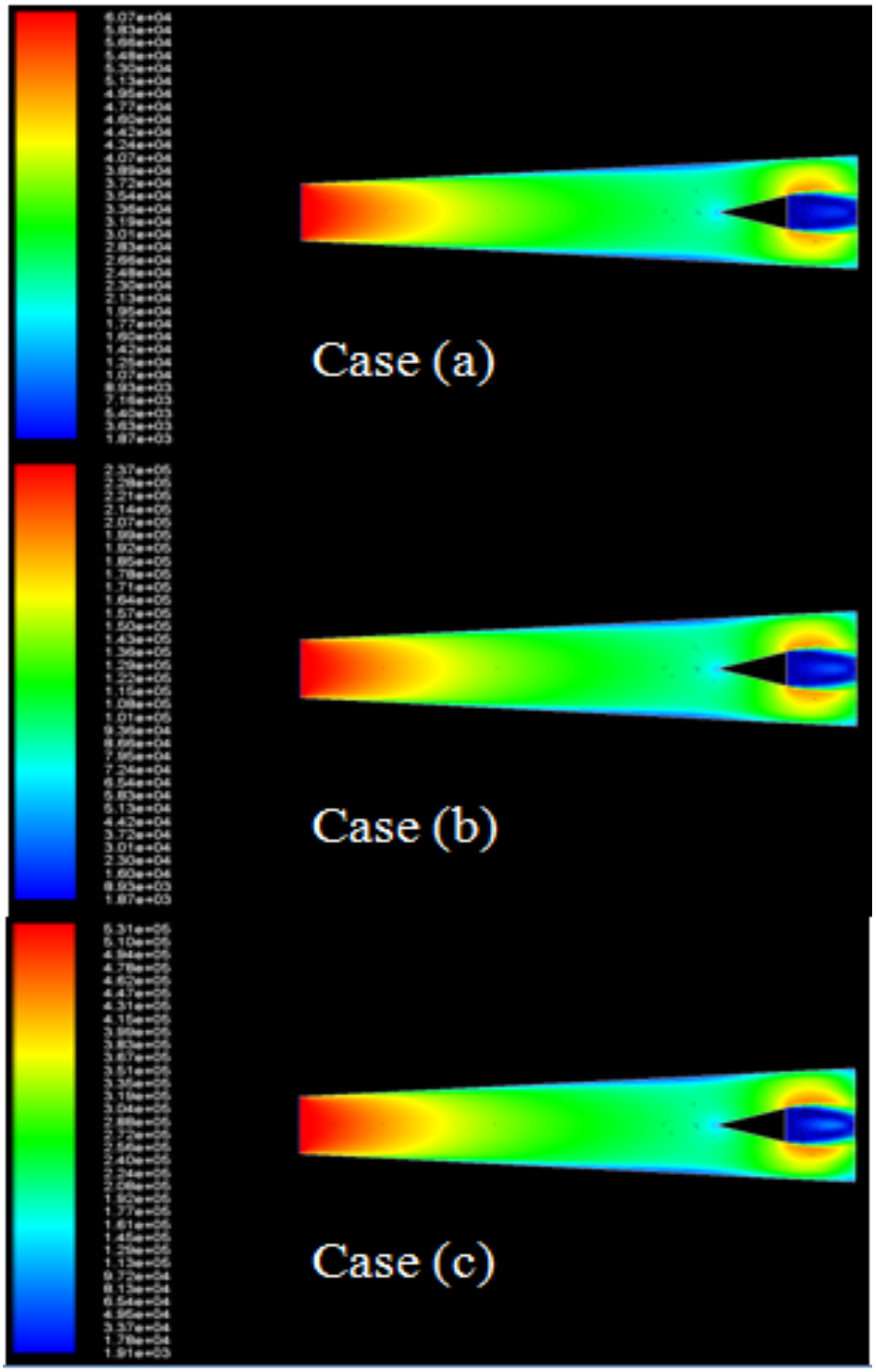

Figure 6: Total Enthalpy simulation of the three cases.

This article is an open access article distributed under the terms and conditions of the Creative Commons Attribution-NonCommercial 4.0 International (CC BY-NC 4.0 license) (http://creativecommons.org/licenses/by-nc/4.0/).

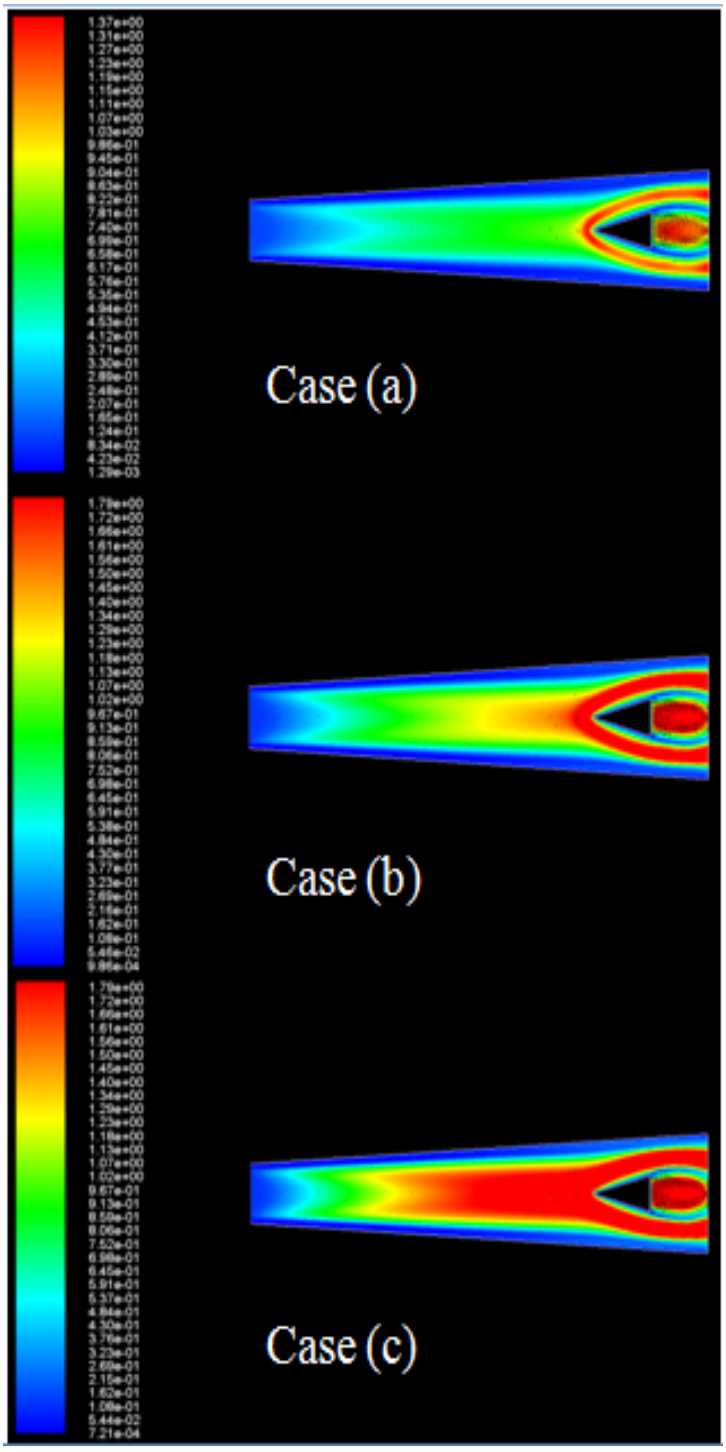

Figure 7: Turbulent viscosity simulation of the three cases.

This article is an open access article distributed under the terms and conditions of the Creative Commons Attribution-NonCommercial 4.0 International (CC BY-NC 4.0 license) (http://creativecommons.org/licenses/by-nc/4.0/).

Conclusions

In this study, the numerical investigation has been perfumed to predict some of the physical properties of an oblique shock wave. Computational fluid dynamics has been used to analyze fluid behavior upstream and downstream of the shock wave. Fine meshing has been used to obtain good resolution. Air has been used as fluid material. The oblique shock wave has been constructed by using a wedge of half-angle $\theta = 22°$ which intercepts the airflow. The study has been performed for three Mach numbers. The continuity equation, momentum equation, and energy equation have been solved numerically. Some of the parameters such as velocity, turbulent viscosity, total pressure, and total enthalpy have been investigated. The measurements revealed that the total pressure downstream of the oblique shock wave is less than that of the upstream shock wave. Furthermore, the total pressure is slightly different for the three cases of Mach numbers. In addition, the turbulent viscosity area around the object becomes thicker as the Mach numbers become bigger. It can be noted that the main conclusion is the oblique shock wave angle ϕ is decreased as the Mach number increases. The differences in the parameters are attributed to the oblique shock wave's influence on the airflow upstream and downstream of the oblique shock wave.

Acknowledgments

The author gratefully acknowledges the Department of Physics, College of Education for Pure Science, University of Basrah.

This article is an open access article distributed under the terms and conditions of the Creative Commons Attribution-NonCommercial 4.0 International (CC BY-NC 4.0 license) (http://creativecommons.org/licenses/by-nc/4.0/).

References

[1] R. Brun, Elements of Gas Dynamics, Introduction to Reactive Gas Dynamics, (2009) 224–258. https://doi.org/10.1093/acprof:oso/9780199552689.003.0010.

[2] J. B. Vemula and K. Sinha, Explicit algebraic Reynolds stress model for shock-dominated flows, Int. J. Heat Fluid Flow, 85(2020)1-15, https://doi.org/10.1016/j.ijheatfluidflow.2020.108680.

[3] Y. G. Ermolaev, A. D. Kosinov, V. L. Kocharin, N. V. Semenov, A. A. Yatskikh, Experimental Investigation of the Weak Shock Wave Influence on the Boundary Layer of a Flat Blunt Plate at the Mach Number 2.5, Fluid Dyn., 54(2019)257–263, https://doi.org/10.1134/S0015462819020058.

[4] G. Della Posta, E. Martelli, P. P. Ciottoli, F. Stella, and M. Bernardini, Enhanced delayed DES of shock wave/boundary layer interaction in a planar transonic nozzle, Int. J. Heat Fluid Flow, 77(2019)359–365, https://doi.org/10.1016/j.ijheatfluidflow.2019.05.001.

[5] X. G. Lu, S. H. Yi, L. He, D. D. Gang, H. B. Niu, Experimental Study on Unsteady Characteristics of Shock and Turbulent Boundary Layer Interactions, Fluid Dyn., 55(2020)566–577, https://doi.org/10.1134/S0015462820030088.

[6] O. Szulc, P. Doerffer, P. Flaszynski, T. Suresh, Numerical modelling of shock wave-boundary layer interaction control by passive wall ventilation, Comput. Fluids, 200(2020)1-21, https://doi.org/10.1016/j.compfluid.2020.104435.

[7] B. John, V. Kulkarni, Numerical assessment of correlations for shock wave boundary layer interaction, Comput. Fluids,90(2014)42–50, https://doi.org/10.1016/j.compfluid.2013.11.011.

[8] Z. Zha, Z. Ye, Z. Hong, K. Ye, Effects of unsteady oblique shock wave on mixing efficiency of two-dimensional supersonic mixing layer, Acta Astronaut.,178(2021) 60–71, https://doi.org/10.1016/j.actaastro.2020.07.028.

[9] Y. Sugiyama, T. Homae, T. Matsumura, and K. Wakabayashi, Numerical investigations on detonations in a condensed-phase explosive and oblique shock waves in surrounding

This article is an open access article distributed under the terms and conditions of the Creative Commons Attribution-NonCommercial 4.0 International (CC BY-NC 4.0 license) (http://creativecommons.org/licenses/by-nc/4.0/).

fluids, Combust. Flame, 211(2020)133–146, https://doi.org/10.1016/j.combustflame.2019.09.025.

[10] A. Zhou, K. Wang, L. Wang, F. Du, Z. Li, Numerical simulation for propagation characteristics of shock wave and gas flow induced by outburst intensity, Int. J. Min. Sci. Technol., 25(215) 107–112, https://doi.org/10.1016/j.ijmst.2014.12.009.

[11] B. Zhao, H. Sun, X. Shi, M. Qi, and S. Guo, Investigation of using multi-shockwave system instead of single normal shock for improving radial inflow turbine reliability, Int. J. Heat Fluid Flow,71(2018)170–178, https://doi.org/10.1016/j.ijheatfluidflow.2018.03.018.

[12] S. Piponniau, E. Collin, P. Dupont, J. francois Debiève, Reconstruction of velocity fields from wall pressure measurements in a shock wave/turbulent boundary layer interaction, Int. J. Heat Fluid Flow, 35(2012)176–186, https://doi.org/10.1016/j.ijheatfluidflow.2012.02.006.

[13] Y. xin Ren, L. Tan, Z. niu Wu, The shape of incident shock wave in steady axisymmetric conical Mach reflection, Adv. Aerodyn.,24(2020)1-11, https://doi.org/10.1186/s42774-020-00047-6.

دراسة عددية لموجة الصدمة المائلة

عامر حسين علي

جامعة البصرة, كلية التربية للعلوم الصرفة, قسم الفيزياء

المستخلص

الهدف من هذه الدراسة هو الكشف عن الخواص الفيزيائية لموجة الصدمة المائلة بطريقة عددية. تم استخدام ديناميكية الموائع الحاسوبية العددية لفهم سلوك الموجة. تم تصميم مجال الحسابات بنظام شبكي دقيق من اجل ضمان الحسابات الدقيقة. تم استخدام الهواء كمادة مائع بسبب كثرة استخداماته في التطبيقات الهندسية. تم استخدام سطح مائل بزاوية $\vartheta = 22^{o}$ امام جريان الهواء ليصنع موجة الصدمة المائلة والتي بدورها تصنع زاوية ϕ. تم اجراء الحسابات لثلاث قيم ماخ , وهي اكبر بقليل لكل من القيم 1 و 2 و 3. كما تم حل معادلات الاستمرارية والزخم والطاقة بطريقة عددية. تم اجراء الحسابات للسرعة واللزوجة والضغط الكلي والانثالبي في مقدمة ومؤخرة موجة الصدمة لقيم ماخ الثلاث. اظهرت النتائج ان الضغط الكلي خلف السطح المائل هي اقل من قيمته في مقدمة السطح المائل كما ان منطقة اللزوجة حول السطح المائل تصبح اكثر سمكا مع زيادة عدد ماخ. الضغط الكلي كان مختلفا قليلا مع قيم ماخ المختلفة. سلوك هذه الخواص التي ذكرت تعود لوجود تأثير موجة الصدمة. تم ملاحظة ان زاوية الصدمة المائلة ϕ تقل بزيادة عدد ماخ.

This article is an open access article distributed under the terms and conditions of the Creative Commons Attribution-NonCommercial 4.0 International (CC BY-NC 4.0 license) (http://creativecommons.org/licenses/by-nc/4.0/).